Mechanism and Machine Theory 133 (2019) 179–194

Contents lists available at ScienceDirect

Mechanism and Machine Theory

journal homepage: www.elsevier.com/locate/mechmachtheory

Research paper

Dynamic modelling and force analysis of a knuckle boom crane using screw theory

Andrej Cibicik*, Olav Egeland

Department of Mechanical and Industrial Engineering, Norwegian University of Science and Technology (NTNU), Trondheim NO-7491, Norway

ARTICLE INFO

Article history:
Received 16 August 2018
Revised 15 October 2018
Accepted 25 October 2018
Available online 28 November 2018

Keywords:
Crane
Dynamic modeling
Force analysis
Reaction force
Robotics
Screw theory

ABSTRACT

This article presents a method for determination of dynamic reaction forces in knuckle boom cranes. The method is based on the dynamic modelling procedure, which is an extension of Kane's equations of motion. An efficient formulation is used, where the link velocities and angular velocities are given in terms of the link twists, which makes it straightforward to describe the partial velocities and partial angular velocities as joint lines given as screws in Plücker coordinates. The method is presented in a systematic and general manner and is applicable for spatial crane-like manipulators with passive rotary joints and piston actuators. We propose a procedure for the substitution of the actual actuator wrenches with an equivalent set of wrenches applied on the actuator supports, which leads to an efficient procedure for the determination of reaction forces in passive joints. The application of screw theory to dynamic modelling and force analysis leads to an elegant and geometrically meaningful formulation. The method is implemented for a knuckle boom crane and simulation results are provided. The determined reaction forces can be used in mechanical problems as structural integrity calculations and fatigue lifetime prediction, as well as in control problems involving dry friction.

1. Introduction

Knuckle boom cranes belong to the class of heavy duty parallel–serial manipulators, which are actuated by prismatic piston actuators, see Fig. 1. This type of actuation is typically used when the requirements for the load capacity are high. The resulting closed-loop structure leads to more complicated dynamic modelling and force analysis procedures than for serial manipulators.

Crane operations in the offshore and maritime industries are of great importance, and require precise and safe motion of crane payloads. Therefore the field of modelling and control of cranes has been widely studied in the research literature [1,2]. When the control of hydraulics is of interest, the hydraulic cylinders are normally included in the dynamic model [3–5]. Alternatively, in theoretical modelling and control studies it may be assumed that the crane is actuated by the joint torques [6,7]. For cranes moving at high speeds the effects of inertial forces of the actuators on the system dynamics become important and they should be included [8]. The reaction forces may be of interest in the analysis of a crane, as they can be

* Corresponding author.
E-mail addresses: andrej.cibicik@ntnu.no (A. Cibicik), olav.egeland@ntnu.no (O. Egeland).

https://doi.org/10.1016/j.mechmachtheory.2018.10.019

Nomenclature

$\boldsymbol{\omega}^i_{0i}$	angular velocity of Body i relative to the inertial frame
$\boldsymbol{\Pi}$	screw interchange operator
$\boldsymbol{\tau}$	vector of generalized external forces
$\breve{\mathsf{W}}_{\mathrm{in}}{}^i_i$, $\breve{\mathsf{W}}_{\mathrm{e}}{}^i_i$, $\breve{\mathsf{W}}_{\mathrm{t}}{}^i_i$	inertial, external and total wrench of Body i with interchanged force and moment vectors
$\mathsf{t}^i_{0i/i}$	twist of Body i relative to the inertial frame, referenced to the origin of Frame i
$\mathsf{W}_{\mathrm{in}}{}^i_i$, $\mathsf{W}_{\mathrm{e}}{}^i_i$, $\mathsf{W}_{\mathrm{t}}{}^i_i$	inertial, external and total wrench of Body i
$\mathsf{W}_{\mathrm{r}}{}^i_i$	reaction wrench in Joint i
$\mathsf{W}^{*bi}_{\mathrm{t}\,bi}$, $\mathsf{W}^{*pi}_{\mathrm{t}\,pi}$	reaction wrench at cylinder barrel bi support, and at cylinder piston pi support
$\bar{\mathbf{R}}^{i+1}_i$	screw coordinate transformation matrix from i to $i+1$
$\mathbf{C}$	Coriolis and centrifugal force matrix of multibody system
$\mathbf{D}_i$	local mass matrix of Body i
$\mathbf{M}$	mass matrix of multibody system
$\mathbf{M}^i_{m_i}$	inertia tensor of Body i
$\mathbf{P}_i$	projection matrix of Body i
$\mathbf{q}$	vector of generalized coordinates
$\mathbf{S}_{bbi}$, $\mathbf{S}_{pbi}$, $\mathbf{S}_{bpi}$, $\mathbf{S}_{ppi}$	auxiliary matrices for derivation of reaction wrenches of cylinder i
$\mathbf{u}$	vector of generalized speeds
$\mathbf{U}^i_{m_i,i}$	screw reference transformation matrix from i to m_i
$\mathbf{v}^i_{0i/i}$	linear velocity of the origin of Frame i relative to the inertial frame
$\mathbf{V}^{i+1,i}_{m_{i+1},i}$	screw transformation matrix, transforms coordinates from i to $i+1$ and transforms reference point from i to m_{i+1}
$\mathbf{W}_i$	auxiliary skew-symmetric matrix of angular velocities of Body i
a_{bi}	distance from Joint i to Frame bi along the axis y_{i-1}
a_{pi}	distance from Joint i to piston pi attachment point along the axis y_i
d_i	COG distance of Body i
e_{bi}	distance from Joint i to Frame bi along the axis z_{i-1}
e_{pi}	distance from Joint i to piston pi attachment point along the axis z_i
l_i	length of Body i
m_i	mass of Body i
α_i	rotation angle from Frame $i-1$ to Frame i
β_i	rotation angle from Frame $i-1$ to Frame bi

used to model joint friction [9]. Moreover, the reaction forces can be used for the structural strength and fatigue analysis of the system under realistic operational scenarios, and for optimal dynamic performance problems [10].

The dynamics of cranes has a much in common with the dynamics of robot manipulators. It is well established that the dynamics of serial manipulators can be modelled with Lagrangian mechanics, which gives valuable insight into the properties of the equations of motion and into the energy of the system [11]. The dynamics can also be modelled with the Newton–Euler formulation, which, in general, will lead to efficient computational schemes. This can be implemented as a recursive Newton–Euler formulation [12], which is used for the inverse dynamics problem, where the generalized forces are computed given the position, velocity and acceleration of the joints. Another method based on the Newton-Euler formulation is Kane's equations of motion [13], which can be used to derive the equations of motion in closed form. Alternatively to formulation using coordinate-free vectors [13], Kane's method can be formulated using column vectors [14] or dual vectors [15], where an angular velocity is a real vector part and a linear velocity is a dual vector part. Both the recursive Newton–Euler scheme and Kane's equations of motion rely on the elimination of the forces of constraint. In Kane's method this is done using partial velocities and partial angular velocities, which can also be formulated with the natural orthogonal complement (NOC) [16,17] or the decomposed NOC [18,19], where the expressions for the NOC can be found directly from the body twists for serial-link manipulators [19]. Kane's method can also be used to bring the forces of constraint into evidence by introducing auxiliary generalized speeds and the corresponding auxiliary partial velocities and auxiliary partial angular velocities [13]. It is noted that there are several other methods for the determination of reaction forces (i.e. forces of constraint) based on Newton–Euler or Lagrangian formalism [20–23]. The dynamic formulation using Lagrange multipliers [24–27] also allows the determination of constraint forces between the system bodies.

In this paper we present a formulation of Kane's equations of motion where the partial velocities and the partial angular velocities are described in terms of the joint twists. This is equivalent to the NOC formulation, with the advantage that the formulation to a larger extent is directly related to the geometry of the problem. Link twists are conveniently derived using screw transformations, which gives a clear geometric interpretation of every step in the derivation. Then the partial

Fig. 1. A down-scaled version of a knuckle boom crane.

velocities and the partial angular velocities will be given as screws describing lines in Plücker coordinates, which can be transformed using screw transformations. The lines of the joints are arranged as the columns of the projection matrices. From the geometric perspective, premultiplication of an external or inertial force with those lines leads to a projection of the force on the line. Moreover, the columns of projection matrices are related to partial velocities in Kane's method [13] and to the columns of the NOC [16,28,29].

The dynamical formulation presented in this paper was used in [6] to derive the equations of motion for a crane-ship system, where a heavy crane is mounted on a ship moving in ocean waves. In the previous work [30] the formulation was used to derive the equations of motion for a serial manipulator and calculate the forces of constraint. In this paper we extend the results of [6,30] to serial-parallel mechanisms with rotary joints and prismatic piston actuators with application to knuckle boom cranes. The dynamical formulation does not require inclusion of constraint equations, and it leads to a minimal set of ODE's. The problem of the closed kinematic loops is solved by the substitution of the actual actuator wrenches applied at the centres of gravity with an equivalent set of wrenches applied at the actuator supports. The modelling procedure is presented in a general manner and is applicable for crane-like manipulators with an arbitrary number of links. Spatial mechanisms can be modelled by combination of links with the actuated rotational joints and the rotational joints actuated by cylinders. The method is also applicable for serial-link manipulators, where the substitution of wrenches is omitted. Reaction forces can be used in mechanical design of mechanisms as well as in control and modelling problems involving dry friction [31,32].

The rest of this paper is organized as follows. Section 2 presents the preliminaries to this work. In Section 3 the dynamic modelling of parallel-serial manipulator arms is discussed, while in Section 4 the method for determination of reaction forces is given. Implementation of the method for a knuckle boom crane is given in Section 5, which is followed by the simulation results and conclusions given in Sections 6 and 7.

2. Preliminaries

2.1. Screws and lines

A screw $\vec{s}_{/B}$ [33,34] is an ordered pair of vectors

$$\vec{s}_{/B} = (\vec{u}, \vec{w}), \tag{1}$$

which satisfies the screw transformation

$$\vec{s}_{/A} = (\vec{u}, \vec{w} + \vec{p}_{AB} \times \vec{u}), \tag{2}$$

where $\vec{s}_{/A}$ is referenced to the point A, $\vec{s}_{/B}$ is referenced to the point B, and $\vec{p}_{AB}$ is the position vector from A to B. A special screw is a line

$$\vec{l}_{/B} = (\vec{a}, \vec{m}), \tag{3}$$

where $\vec{a}$ is the unit direction vector of the line, and $\vec{m} = \vec{p} \times \vec{a}$ is the moment of the line, where $\vec{p}$ is the position vector from the reference point B to any point on the line. It is noted that the direction vector $\vec{a}$ and the moment $\vec{m}$ are orthogonal.

A screw $\vec{s}_{/B}$ is said to have the line $\vec{l}_{/B}$ as its screw axis if it can be written

$$\vec{s}_{/B} = \alpha(\vec{a}, \vec{m} + h\vec{a}), \tag{4}$$

where α is a real scalar and h is a pitch of the screw. It follows that a line is a screw with zero pitch. The screw $\vec{\lambda} = (\vec{0}, \vec{a})$ has infinite pitch, and is said to be a line at infinity.

The coordinate form of a screw is written

$$\mathrm{s}^j_{/b} = \begin{bmatrix} \mathbf{u}^j \\ \mathbf{w}^j \end{bmatrix}, \tag{5}$$

where $\mathbf{u}^j$ and $\mathbf{w}^j$ are vectors given in the coordinates of Frame j. The screw transformation from a screw with reference in the origin of Frame b and coordinates in j to the same screw with reference to the origin of Frame a and coordinates in i is given by

$$\mathrm{s}^i_{/a} = \bar{\mathbf{R}}^i_j \mathbf{U}^j_{ab} \mathrm{s}^j_{/b}, \tag{6}$$

where the screw rotation matrix $\bar{\mathbf{R}}^i_j$ transforms the coordinates from j to i, and is given by

$$\bar{\mathbf{R}}^i_j = \begin{bmatrix} \mathbf{R}^i_j & \mathbf{0} \\ \mathbf{0} & \mathbf{R}^i_j \end{bmatrix}, \tag{7}$$

where $\mathbf{R}^i_j \in SO(3)$ is an orthogonal rotation matrix [11] from i to j. The screw reference transformation matrix $\mathbf{U}^j_{ab}$ changes the point of reference from b to a, and is given by

$$\mathbf{U}^j_{ab} = \begin{bmatrix} \mathbf{I} & \mathbf{0} \\ \hat{\mathbf{p}}^j_{ab} & \mathbf{I} \end{bmatrix}, \tag{8}$$

where $\mathbf{p}^j_{ab}$ is the position vector from a to b in the coordinates of j. The notation $\hat{\cdot}$ denotes the skew-symmetric form of a vector. It is noted that

$$\bar{\mathbf{R}}^i_j \mathbf{U}^j_{ab} = \begin{bmatrix} \mathbf{R}^i_j & \mathbf{0} \\ \hat{\mathbf{p}}^i_{ab}\mathbf{R}^i_j & \mathbf{R}^i_j \end{bmatrix}, \tag{9}$$

where $\mathbf{R}^i_j \hat{\mathbf{p}}^j_{ab} = \hat{\mathbf{p}}^i_{ab}\mathbf{R}^i_j$, the term (9) is referred as a screw transformation matrix in [34]. The resulting screw referenced to a is

$$\mathrm{s}^i_{/a} = \begin{bmatrix} \mathbf{u}^i \\ \mathbf{w}^i + \hat{\mathbf{p}}^i_{ab}\mathbf{u}^i \end{bmatrix}. \tag{10}$$

2.2. Twists

The displacement of Frame j relative to Frame i is given by the homogeneous transformation matrix [11]

$$\mathbf{T}^i_j = \begin{bmatrix} \mathbf{R}^i_j & \mathbf{p}^i_{ij} \\ \mathbf{0}^\mathrm{T} & 1 \end{bmatrix}. \tag{11}$$

The corresponding twist of Frame j relative to Frame i referenced to the origin of Frame j is then [33,35]

$$\mathrm{t}^j_{ij/j} = \begin{bmatrix} \boldsymbol{\omega}^j_{ij} \\ \mathbf{v}^j_{ij/j} \end{bmatrix}. \tag{12}$$

This twist is related to the time derivative of the displacement $\mathbf{T}^i_j$ according to $\dot{\mathbf{T}}^i_j = \mathbf{T}^i_j \hat{\mathrm{t}}^j_{ij/j}$, where

$$\hat{\mathrm{t}}^j_{ij/j} = (\mathbf{T}^i_j)^{-1}\dot{\mathbf{T}}^i_j = \begin{bmatrix} \hat{\boldsymbol{\omega}}^j_{ij} & \mathbf{v}^j_{ij/j} \\ \mathbf{0}^\mathrm{T} & 0 \end{bmatrix} \tag{13}$$

is the matrix form of the twist $\mathrm{t}^j_{ij/j}$. It is seen that $\hat{\boldsymbol{\omega}}^j_{ij} = (\mathbf{R}^i_j)^\mathrm{T}\dot{\mathbf{R}}^i_j$ is the angular velocity of j relative to i, and $\mathbf{v}^j_{ij/j} = (\mathbf{R}^i_j)^\mathrm{T}\dot{\mathbf{p}}^i_{ij}$ is the velocity of j relative to i.

If the twist is given as $\mathrm{t}^i_{ij/i}$, which is the same twist referenced to Frame i and given in the coordinates of i, then $\dot{\mathbf{T}}^i_j = \hat{\mathrm{t}}^i_{ij/i}\mathbf{T}^i_j$ and $\mathrm{t}^i_{ij/i} = [(\boldsymbol{\omega}^i_{ij})^\mathrm{T}, (\mathbf{v}^i_{ij/i})^\mathrm{T}]^\mathrm{T}$, where $\mathbf{v}^i_{ij/i}$ is the velocity a point fixed in Frame j that passes through the origin of Frame i. Assume the particular case where the displacement is a rotation θ_i about a unit vector $\mathbf{a}^i$ through the origin of i, then it follows that $\mathbf{v}^i_{ij/i} = \mathbf{0}$, and the twist is simply

$$\mathsf{t}^i_{ij/i} = \begin{bmatrix} \dot{\theta}\mathbf{a}^i \\ \mathbf{0} \end{bmatrix} = \dot{\theta}\mathsf{L}^i_{i/i}, \tag{14}$$

where $\mathsf{L}^i_{i/i} = [(\mathbf{a}^i)^\mathrm{T}, \mathbf{0}^\mathrm{T}]^\mathrm{T}$ is the line with the direction vector $\mathbf{a}^i$ through the origin of i. Note that this line is a screw, which satisfies screw transformations. If the motion of Frame j is instead a translation d along $\mathsf{L}^i_{i/i}$, then the twist is

$$\mathsf{t}^i_{ij/i} = \begin{bmatrix} \mathbf{0} \\ \dot{d}\mathbf{a}^i \end{bmatrix} = \dot{d}\boldsymbol{\lambda}^i_{i/i}, \tag{15}$$

where $\boldsymbol{\lambda}^i_{i/i} = [\mathbf{0}^\mathrm{T}, (\mathbf{a}^i)^\mathrm{T}]^\mathrm{T}$ is the line at infinity.

It is noted that the twist $\mathsf{t}^k_{ik/k}$ of a composite displacement $\mathbf{T}^i_k = \mathbf{T}^i_j\mathbf{T}^j_k$ is given by its matrix form

$$\hat{\mathsf{t}}^k_{ik/k} = \mathbf{T}^k_i\dot{\mathbf{T}}^i_k = \mathbf{T}^k_j\mathbf{T}^j_i\dot{\mathbf{T}}^i_j\mathbf{T}^j_k + \mathbf{T}^k_j\dot{\mathbf{T}}^j_k = \hat{\mathsf{t}}^k_{ij/k} + \hat{\mathsf{t}}^k_{jk/k},$$

where it is used that $\hat{\mathsf{t}}^k_{ij/k} = \mathbf{T}^k_j\hat{\mathsf{t}}^j_{ij/j}\mathbf{T}^j_k$, which is verified by direct computation. This means that the twist of the composite displacement is the sum of the twists of the individual displacements, that is

$$\mathsf{t}^k_{ik/k} = \mathsf{t}^k_{ij/k} + \mathsf{t}^k_{jk/k}. \tag{16}$$

Note that the twists must be referenced to origin of the same frame, and must be given in the coordinates of the same frame in this summation.

2.3. Dynamics of serial manipulators

A dynamical model of a serial-link manipulator can be derived by, firstly, defining free-body dynamics of every Link k and, secondly, deriving the constrained equation of motion using the NOC [16], projection matrices [30], partial velocities [13] or other similar approaches. Twists can be used both for deriving the free-body dynamics and for defining the velocity constraints between the manipulator links. Twists can be linked to the screw notations and can be transformed using screw transformations while retaining the geometrical meaning of mathematical manipulations.

Following the procedure given in details in [30] we define a twist of Link k relative to the inertial frame, referenced to the origin of Frame k and expressed in the coordinates of Frame k as

$$\mathsf{t}^k_{0k/k} = \begin{bmatrix} \boldsymbol{\omega}^k_{0k} \\ \mathbf{v}^k_{0k/k} \end{bmatrix}, \tag{17}$$

where the twist $\mathsf{t}^k_{0k/k}$ is a screw. The twist (17) can be transformed to be referenced to the COG point m_k (centre of gravity of Link k) and to the origin of Frame $k+1$ (Link $k+1$ body-fixed frame) by screw transformations. The transformed twist is the same line, just given from the view of a different reference point

$$\mathsf{t}^k_{0k/m_k} = \mathbf{U}^k_{m_k,k}\mathsf{t}^k_{0k/k}, \quad \mathsf{t}^k_{0k/k+1} = \mathbf{U}^k_{k+1,k}\mathsf{t}^k_{0k/k}, \tag{18}$$

where $\mathbf{U}^k_{m_k,k}$ and $\mathbf{U}^k_{k+1,k}$ are the screw reference transformation matrices

$$\mathbf{U}^k_{m_k,k} = \begin{bmatrix} \mathbf{I} & \mathbf{0} \\ \hat{\mathbf{p}}^k_{m_k,k} & \mathbf{I} \end{bmatrix}, \quad \mathbf{U}^k_{k+1,k} = \begin{bmatrix} \mathbf{I} & \mathbf{0} \\ \hat{\mathbf{p}}^k_{k+1,k} & \mathbf{I} \end{bmatrix}. \tag{19}$$

The term $\hat{\mathbf{p}}^k_{m_k,k}$ is a skew-symmetric form of the position vector $\mathbf{p}^k_{m_k,k}$ from the COG point m_k to the origin of Frame k, expressed in the coordinates of Frame k. The term $\hat{\mathbf{p}}^k_{k+1,k}$ is defined analogically. The twist $\mathsf{t}^k_{0k/k+1}$ (18) can be expressed in the coordinates of Frame $k+1$ by the coordinate transformation

$$\mathsf{t}^{k+1}_{0k/k+1} = \bar{\mathbf{R}}^{k+1}_k\mathsf{t}^k_{0k/k+1}, \tag{20}$$

where $\bar{\mathbf{R}}^{k+1}_k$ is given by

$$\bar{\mathbf{R}}^{k+1}_k = \begin{bmatrix} \mathbf{R}^{k+1}_k & \mathbf{0} \\ \mathbf{0} & \mathbf{R}^{k+1}_k \end{bmatrix}. \tag{21}$$

A simultaneous transformation of the reference and coordinates can be obtained by

$$\mathsf{t}^{k+1}_{0k/k+1} = \bar{\mathbf{R}}^{k+1}_k\mathbf{U}^k_{k+1,k}\mathsf{t}^k_{0k/k} = \begin{bmatrix} \mathbf{R}^{k+1}_k & \mathbf{0} \\ \mathbf{R}^{k+1}_k\hat{\mathbf{p}}^k_{k+1,k} & \mathbf{R}^{k+1}_k \end{bmatrix}\mathsf{t}^k_{0k/k}, \tag{22}$$

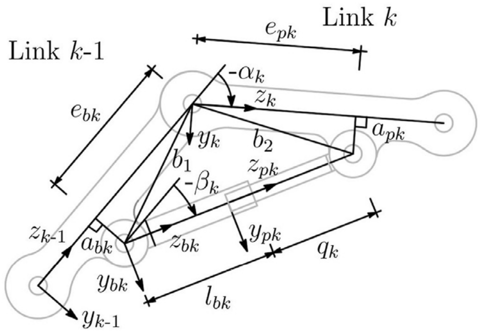

Fig. 2. A two-link system with a passive joint and a cylinder.

where the transformation of the type $\bar{\mathbf{R}}_k^{k+1}\mathbf{U}_{k+1,k}^k$ is also referred as an adjoint transformation. The twist (22) can additionally be referenced to the COG of Link $k+1$ by the screw transformation

$$\mathrm{t}_{0k/m_{k+1}}^{k+1} = \mathbf{U}_{m_{k+1},k+1}^{k+1}\bar{\mathbf{R}}_k^{k+1}\mathbf{U}_{k+1,k}^k\mathrm{t}_{0k/k}^k = \mathbf{V}_{m_{k+1},k}^{k+1,k}\mathrm{t}_{0k/k}^k, \tag{23}$$

where

$$\mathbf{V}_{m_{k+1},k}^{k+1,k} = \begin{bmatrix} \mathbf{R}_k^{k+1} & \mathbf{0} \\ \hat{\mathbf{p}}_{m_{k+1},k+1}^{k+1}\mathbf{R}_k^{k+1} + \mathbf{R}_k^{k+1}\hat{\mathbf{p}}_{k+1,k}^k & \mathbf{R}_k^{k+1} \end{bmatrix}. \tag{24}$$

Twists expressed in the coordinates of the same frame and references to the same point can be summed up as in (16)

$$\mathrm{t}_{0,k+1/m_{k+1}}^{k+1} = \mathrm{t}_{0k/m_{k+1}}^{k+1} + \mathrm{t}_{k,k+1/m_{k+1}}^{k+1}. \tag{25}$$

The twist of Link k t_{0k/m_k}^k can be expressed as

$$\mathrm{t}_{0k/m_k}^k = \mathbf{P}_k\mathbf{u} \tag{26}$$

and its derivative with respect to time can be expressed as

$$\dot{\mathrm{t}}_{0k/m_k}^k = \mathbf{P}_k\dot{\mathbf{u}} + \dot{\mathbf{P}}_k\mathbf{u}, \tag{27}$$

where $\mathbf{P}_k$ is a projection matrix of Link k

$$\mathbf{P}_k = \frac{\partial \mathrm{t}_{0k/m_k}^k}{\partial \mathbf{u}} \tag{28}$$

and $\mathbf{u}$ is a vector of generalized speeds [13]. The nonzero columns of the projection matrix are the joint lines, referenced to the COG of Link k. For the rest of the dynamic modelling procedure of a serial manipulator the reference is made to the previous publication [30].

The method of auxiliary generalized speeds for determination of reaction forces can be efficiently implemented using twists for a serial manipulator. However for closed-loop systems, the implementation becomes rather complex. Therefore, in this work we propose an alternative method, which is specifically formulated for knuckle boom cranes and similar robotic manipulators.

3. Modelling of parallel–serial manipulator arms

3.1. Kinematic constraints in the closed loop

We present the modelling procedure in a general manner, such that it can be applied both for knuckle boom cranes and for similar robot manipulators with an arbitrary number of links. Consider a two-link mechanical unit with a prismatic actuator (which will be referred as *a cylinder* in the rest of this paper) shown in Fig. 2. By application of the cosine rule we can easily derive the kinematic relations between the piston extension q_k and the angles α_k, β_k. The rotation angle α_k from Frame $k-1$ to Frame k is

$$\alpha_k = \arccos\frac{(l_{bk}+q_k)^2 - b_1^2 - b_2^2}{-2b_1b_2} + \arctan\frac{a_{bk}}{e_{bk}} + \arctan\frac{a_{pk}}{e_{pk}} - \pi, \tag{29}$$

where $b_1^2 = a_{bk}^2 + e_{bk}^2$ and $b_2^2 = a_{pk}^2 + e_{pk}^2$. The rotation angle β_k from Frame $k-1$ to Frame bk is

$$\beta_k = -\arccos\frac{b_2^2 - b_1^2 - (l_{bk}+q_k)^2}{-2b_1(l_{bk}+q_k)} - \arctan\frac{e_{bk}}{a_{bk}} + \frac{\pi}{2}. \tag{30}$$

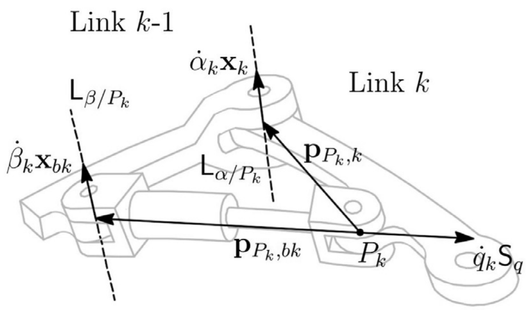

Fig. 3. A two-link system actuated by a cylinder. The line L_α defines the rotation axis of Joint k, the line L_β defines the rotation axis of the cylinder joint and the screw S_q defines the translational direction of the cylinder piston.

Analytic expressions for rotation rates $\dot{\alpha}_k(q, \dot{q})$ and $\dot{\beta}_k(q, \dot{q})$ can be derived by differentiation of (29) and (30) with respect to time. However, in this paper we will demonstrate a geometric approach, which is formulated using screws and screw transformations. In certain cases a geometric procedure leads to the easier mathematical derivation of closed-form expressions compared to time differentiation.

Consider the same two-link system given in Fig. 3, where Link $k-1$ is fixed in space, while Link k and the cylinder are attached to Link $k-1$. The line $\mathsf{L}^k_{\alpha/P_k}$ defines the positive rotational direction of the joint of Link k. When the line is referenced to the point P_k it is given by

$$\mathsf{L}^k_{\alpha/P_k} = \begin{bmatrix} \mathbf{x}^k_k \\ \hat{\mathbf{p}}^k_{P_k,k} \mathbf{x}^k_k \end{bmatrix} = \begin{bmatrix} 1 & 0 & 0 & 0 & -e_{pk} & a_{pk} \end{bmatrix}^{\mathrm{T}}. \tag{31}$$

The line $\mathsf{L}^{bk}_{\beta/P_k}$ defines the positive rotational direction of the joint of the cylinder and when it is referenced to the point P_k it is given by

$$\mathsf{L}^{bk}_{\beta/P_k} = \begin{bmatrix} \mathbf{x}^{bk}_{bk} \\ \hat{\mathbf{p}}^{bk}_{P_k,bk} \mathbf{x}^{bk}_{bk} \end{bmatrix} = \begin{bmatrix} 1 & 0 & 0 & 0 & -(l_{bk} + q_k) & 0 \end{bmatrix}^{\mathrm{T}}, \tag{32}$$

where l_{bk} and q_k are given in Fig. 2. The screw with infinite pitch S^{bk}_q defines the positive translational direction of the piston

$$\mathsf{S}^{bk}_q = \begin{bmatrix} \mathbf{0} \\ \mathbf{z}^{bk}_{bk} \end{bmatrix} = \begin{bmatrix} 0 & 0 & 0 & 0 & 0 & 1 \end{bmatrix}^{\mathrm{T}}. \tag{33}$$

Premultiplication of (31), (32) and (33) with the corresponding rates $\dot{\alpha}_k$, $\dot{\beta}_k$ and $\dot{q}_k$ gives twists associated with the joint lines. The virtual work of some wrench W_i, which is compatible with the reactions in the joint P_k, on the cylinder twist referenced to the point P_k is equal to the virtual work of the same wrench on the Link k twist referenced to the point P_k. Consider a unit wrench [33,36]

$$\mathsf{W}^{bk}_1 = \begin{bmatrix} 0 & 0 & 1 & 0 & 0 & 0 \end{bmatrix}^{\mathrm{T}}, \tag{34}$$

then the virtual work equation is written as

$$\mathsf{W}^{bk}_1 \mathbf{\Pi} (\mathsf{L}^{bk}_{\beta/P_k} \dot{\beta}_k + \mathsf{S}^{bk}_q \dot{q}_k)\ \delta t = \mathsf{W}^{bk}_1 \mathbf{\Pi} \bar{\mathbf{R}}^{bk}_k \mathsf{L}^k_{\alpha/P_k} \dot{\alpha}_k\ \delta t, \tag{35}$$

where δt is an infinitesimal increment of time, $\bar{\mathbf{R}}^{bk}_k$ is given by (21) and

$$\mathbf{\Pi} = \begin{bmatrix} \mathbf{0} & \mathbf{I} \\ \mathbf{I} & \mathbf{0} \end{bmatrix} \tag{36}$$

is an interchange operator [33]. Eq. (35) can be solved in terms of $\dot{\alpha}_k$

$$\dot{\alpha}_k(q_k, \dot{q}_k) = \frac{1}{a_{pk} c_{\alpha\beta k} - e_{pk} s_{\alpha\beta k}} \dot{q}_k, \tag{37}$$

where e_{pk}, a_{pk} are given in Fig. 2 and $c_{\alpha\beta_k} = \cos(\alpha_k - \beta_k)$, $s_{\alpha\beta k} = \sin(\alpha_k - \beta_k)$. Consider a different normalized wrench

$$\mathsf{W}^{bk}_2 = \begin{bmatrix} 0 & 1 & 0 & 0 & 0 & 0 \end{bmatrix}^{\mathrm{T}}, \tag{38}$$

then the virtual work equation is written as

$$\mathsf{W}^{bk}_2 \mathbf{\Pi} \left(\mathsf{L}^{bk}_{\beta/P_k} \dot{\beta}_k + \mathsf{S}^{bk}_q \dot{q}_k\right)\ \delta t = \mathsf{W}^{bk}_2 \mathbf{\Pi} \bar{\mathbf{R}}^{bk}_k \mathsf{L}^k_{\alpha/P_k} \dot{\alpha}_k\ \delta t, \tag{39}$$

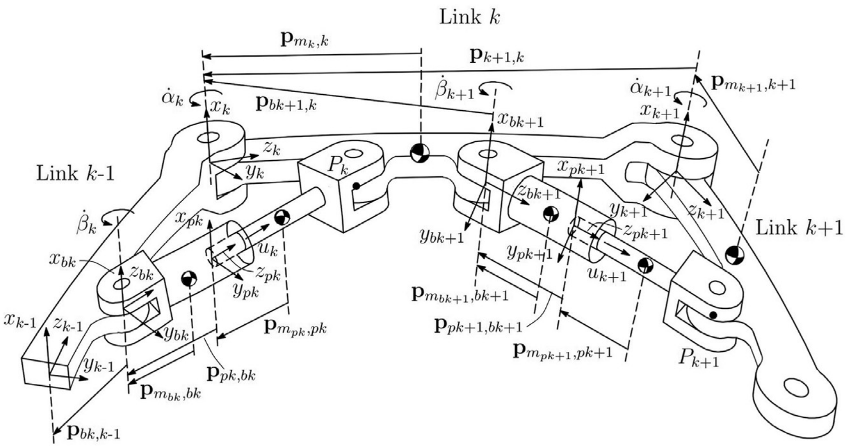

Fig. 4. A part of a serial manipulator actuated by cylinders.

which can be solved in terms of $\dot{\beta}_k$

$$\dot{\beta}_k(q_k, \dot{q}_k) = \frac{e_{pk}c_{\alpha\beta k} + a_{pk}s_{\alpha\beta k}}{l_{bk} + q_k}\dot{\alpha}_k = \frac{e_{pk}c_{\alpha\beta k} + a_{pk}s_{\alpha\beta k}}{(l_{bk} + q_k)(a_{pk}c_{\alpha\beta k} - e_{pk}s_{\alpha\beta k})}\dot{q}_k, \tag{40}$$

where (37) is substituted for $\dot{\alpha}_k$ and l_{bk} is given in Fig. 2.

3.2. System configuration and equations of motion

In this section we will derive the equations of motion in a general manner, such that the procedure can be implemented for a crane-like manipulator with arbitrary number of links. A general part of such manipulator is given in Fig. 4. The system consists of n rigid links with n passive revolute joints and n cylinders for joint actuation. Each rigid Link k has a length l_k, a mass m_k and a distance d_k from the COG (centre of gravity) to the origin of Frame k, which is a body-fixed frame. Each cylinder k consists of a barrel bk and a piston pk, which have lengths l_{bk}, l_{pk} and masses m_{bk}, m_{pk} respectively. A distance d_{bk} is measured from the COG of a barrel bk to the origin of Frame bk, which is a body-fixed frame. However for a piston pk a distance d_{pk} is measured from the COG to the piston attachment point P_k, see Fig. 4.

The configuration space of the system is defined by the vector of generalized coordinates $\mathbf{q}$ [11], while the main variables in the system are generalized speeds [13] which are given by the vector $\mathbf{u}$

$$\mathbf{q} = \begin{bmatrix} q_1 & \cdots & q_k & \cdots & q_n \end{bmatrix}^{\mathrm{T}}, \quad \mathbf{u} = \begin{bmatrix} u_1 & \cdots & u_k & \cdots & u_n \end{bmatrix}^{\mathrm{T}}, \tag{41}$$

where $u_k = \dot{q}_k$. To obtain twists for the system bodies we break the constraint at the piston attachment point P_k. That enables us to implement the procedure for a serial manipulator given in preliminaries. The orientation and rotational speed $\alpha_k, \dot{\alpha}_k$ of Joint k are given as a function of the piston extension and piston linear speed $q_k, \dot{q}_k$ (29), (37). Similarly, the orientation and rotational speed $\beta_k, \dot{\beta}_k$ of Joint bk are given as a function of the piston extension and piston linear speed $q_k, \dot{q}_k$ (30), (40).

The necessary screw reference transformation matrices $\mathbf{U}_{ij}$ (19) are derived using position vectors $\mathbf{p}_{ij}$, which are specified in Fig. 4.

The next step is to obtain the projection matrices (28) for the links, cylinder barrels and cylinder pistons $\mathbf{P}_k$, $\mathbf{P}_{bk}$ and $\mathbf{P}_{pk}$. Note that the workless reaction forces are vanished from the equations of motion by the principle of virtual work [13,37]

$$\sum_i \mathbf{P}_i^{\mathrm{T}} \begin{bmatrix} \mathbf{n}_i^{i(c)} \\ \mathbf{f}_i^{i(c)} \end{bmatrix} = 0, \tag{42}$$

where $\mathbf{n}_i^{i(c)}$ are the reaction moments, $\mathbf{f}_i^{i(c)}$ are the reaction forces and $i = k, bk, pk$ for $k = 1 \cdots n$. Then the equations of motion for a multibody system can be formulated by

$$\mathbf{M}\dot{\mathbf{u}} + \mathbf{C}\mathbf{u} = \boldsymbol{\tau}, \tag{43}$$

where

$$\begin{aligned}\mathbf{M} &= \sum_{k} \mathbf{P}_k^{\mathrm{T}} \mathbf{D}_k \mathbf{P}_k + \sum_{bk} \mathbf{P}_{bk}^{\mathrm{T}} \mathbf{D}_{bk} \mathbf{P}_{bk} + \sum_{pk} \mathbf{P}_{pk}^{\mathrm{T}} \mathbf{D}_{pk} \mathbf{P}_{pk}, \\ \mathbf{C} &= \sum_{k} \mathbf{P}_k^{\mathrm{T}} \left[\mathbf{D}_k \dot{\mathbf{P}}_k + \mathbf{W}_k \mathbf{D}_k \mathbf{P}_k \right] + \sum_{bk} \mathbf{P}_{bk}^{\mathrm{T}} \left[\mathbf{D}_{bk} \dot{\mathbf{P}}_{bk} + \mathbf{W}_{bk} \mathbf{D}_{bk} \mathbf{P}_{bk} \right] \\ &\quad + \sum_{pk} \mathbf{P}_{pk}^{\mathrm{T}} \left[\mathbf{D}_{pk} \dot{\mathbf{P}}_{pk} + \mathbf{W}_{pk} \mathbf{D}_{pk} \mathbf{P}_{pk} \right]\end{aligned} \tag{44}$$

and

$$\mathbf{D}_i = \begin{bmatrix} \mathbf{M}_{m_i}^i & \mathbf{0} \\ \mathbf{0} & m_i \mathbf{I} \end{bmatrix}, \quad \mathbf{W}_i = \begin{bmatrix} \hat{\omega}_{0i}^i & \mathbf{0} \\ \mathbf{0} & \hat{\omega}_{0i}^i \end{bmatrix}, \tag{45}$$

where $i = k, bk, pk$ for $k = 1 \cdots n$. The matrices $\mathbf{M}$ and $\mathbf{C}$ have the property that $(\dot{\mathbf{M}} - 2\mathbf{C})$ is a skew-symmetric matrix [11,37]. The vector of generalized external forces is given by

$$\boldsymbol{\tau} = \sum_{k} \mathbf{P}_k^{\mathrm{T}} \boldsymbol{\Pi} \mathrm{W_e}_k^k + \sum_{bk} \mathbf{P}_{bk}^{\mathrm{T}} \boldsymbol{\Pi} \mathrm{W_e}_{bk}^{bk} + \sum_{pk} \mathbf{P}_{pk}^{\mathrm{T}} \boldsymbol{\Pi} \mathrm{W_e}_{pk}^{pk}, \tag{46}$$

where $\mathrm{W_e}_i^i = \left[\mathbf{f}_{m_i}^{i\mathrm{T}} \quad \mathbf{n}_{m_i}^{i\mathrm{T}} \right]^{\mathrm{T}}$ is the wrench of resultant external effects, $\mathbf{n}_{m_i}^i$ is the resulting moment on Body i and $\mathbf{f}_{m_i}^i$ is the resulting force applied at the COG of Body i. The matrix $\boldsymbol{\Pi}$ is an interchange operator (36), which leads to the new wrench notation [33] $\breve{\mathrm{W}}_i = \boldsymbol{\Pi} \mathrm{W}_i$.

4. Reaction forces

4.1. Inertial and external wrenches

Once the equations of motion (43) are solved, the wrench of the resultant inertial effects $\mathrm{W_{in}}_i^i$ for Body i, applied at the COG of Body i and expressed in the coordinates of Frame i can be derived using twist notations

$$\breve{\mathrm{W}}_{\mathrm{in}_i}^i = \mathbf{D}_i \dot{\mathrm{t}}_{0i/m_i}^i + \mathbf{W}_i \mathbf{D}_i \mathrm{t}_{0i/m_i}^i. \tag{47}$$

Substitution of (26) and (27) into (47) leads to

$$\breve{\mathrm{W}}_{\mathrm{in}_i}^i = \mathbf{D}_i \mathbf{P}_i \dot{\mathbf{u}} + (\mathbf{D}_i \dot{\mathbf{P}}_i + \mathbf{W}_i \mathbf{D}_i \mathbf{P}_i) \mathbf{u}, \tag{48}$$

where the index $i = k, bk, pk$ for $k = 1 \cdots n$. The total wrench acting at the COG of Body i is found as a difference of external and inertial wrenches

$$\breve{\mathrm{W}}_{\mathrm{t}_i}^i = \breve{\mathrm{W}}_{\mathrm{e}_i}^i - \breve{\mathrm{W}}_{\mathrm{in}_i}^i, \tag{49}$$

where $\breve{\mathrm{W}}_{\mathrm{in}_i}^i$ is obtained by (48) and $\breve{\mathrm{W}}_{\mathrm{e}_i}^i$ is the same as in (46). Considering the interchange operator (36), the following equalities hold

$$\mathrm{W}_{\mathrm{in}_i}^i = \boldsymbol{\Pi} \breve{\mathrm{W}}_{\mathrm{in}_i}^i, \quad \mathrm{W}_{\mathrm{e}_i}^i = \boldsymbol{\Pi} \breve{\mathrm{W}}_{\mathrm{e}_i}^i, \quad \mathrm{W}_{\mathrm{t}_i}^i = \boldsymbol{\Pi} \breve{\mathrm{W}}_{\mathrm{t}_i}^i. \tag{50}$$

4.2. Equivalent cylinder wrenches

In this section we derive a set of cylinder wrenches applied at the cylinder supports, which is equivalent to the initial set of wrenches applied at the COGs. The initial cylinder wrenches for the barrel and the piston are derived by (49) and (50).

4.2.1. Axial reactions

The mathematical model of the cylinder adapted in this work is invariant with the type of primary actuation source (i.e. hydraulic oil, mechanical actuation, etc). That is the cylinder is actuated by a point force applied on the piston along the longitudinal z_{pk} axis and the opposite force of the same magnitude applied on the barrel. In such mathematical model, where there is no mechanical constraints along the longitudinal axis, the axial inertial force on the piston will be fully transferred to the piston support and the axial inertial force on the barrel will be fully transferred to the barrel support.

4.2.2. Transverse reactions

The transverse cylinder reactions on the supports can be found from the wrench equilibrium equations. Assume that $\mathrm{W}_{\mathrm{t}\,bk}^{*}$ and $\mathrm{W}_{\mathrm{t}\,pk}^{*}$ are the reaction wrenches applied at the cylinder supports, then the equilibrium equation of the wrenches referenced to origin of Frame bk is

$$\mathrm{W}_{\mathrm{t}\,bk}^{*bk} + \mathbf{U}_{bk,P_k}^{pk} \mathrm{W}_{\mathrm{t}\,pk}^{*pk} = \mathbf{U}_{bk,m_{bk}}^{bk} \mathrm{W}_{\mathrm{t}\,bk}^{bk} + \mathbf{U}_{bk,m_{pk}}^{pk} \mathrm{W}_{\mathrm{t}\,pk}^{pk}, \tag{51}$$

which gives six equation, where equations four and five together with the considerations in the previous subsection are solved for the components of $\mathrm{W}^{*\,pk}_{\mathrm{t}\,pk}$. The equilibrium equation of the same wrenches referenced to the piston support P_k is

$$\mathbf{U}^{bk}_{P_k,bk}\mathrm{W}^{*\,bk}_{\mathrm{t}\,bk} + \mathrm{W}^{*\,pk}_{\mathrm{t}\,pk} = \mathbf{U}^{bk}_{P_k,m_{bk}}\mathrm{W}_{\mathrm{t}\,bk}^{\,bk} + \mathbf{U}^{pk}_{P_k,m_{pk}}\mathrm{W}_{\mathrm{t}\,pk}^{\,pk}, \tag{52}$$

which also gives six equation, where equations four, five and six, together with the considerations in the previous subsection, are solved for the components of $\mathrm{W}^{*\,bk}_{\mathrm{t}\,bk}$. The results obtained in (51) and (52) are formalized in a more convenient form

$$\begin{aligned} \mathrm{W}^{*\,bk}_{\mathrm{t}\,bk} &= \mathbf{S}_{bbk}\mathrm{W}_{\mathrm{t}\,bk}^{\,bk} + \mathbf{S}_{pbk}\mathrm{W}_{\mathrm{t}\,pk}^{\,pk}, \\ \mathrm{W}^{*\,pk}_{\mathrm{t}\,pk} &= \mathbf{S}_{bpk}\mathrm{W}_{\mathrm{t}\,bk}^{\,bk} + \mathbf{S}_{ppk}\mathrm{W}_{\mathrm{t}\,pk}^{\,pk}, \end{aligned} \tag{53}$$

where the proposed auxiliary matrices $\mathbf{S}_{ijk}$ are defined as

$$\mathbf{S}_{bbk} = \left[\begin{array}{cccccc} \frac{l_{ck}-d_{bk}}{l_{ck}} & 0 & 0 & 0 & -\frac{1}{l_{ck}} & 0 \\ 0 & \frac{l_{ck}-d_{bk}}{l_{ck}} & 0 & \frac{1}{l_{ck}} & 0 & 0 \\ 0 & 0 & 1 & 0 & 0 & 0 \\ \multicolumn{6}{c}{\mathbf{0}_{2\times 6}} \\ 0 & 0 & 0 & 0 & 0 & 1 \end{array}\right], \quad \mathbf{S}_{pbk} = \left[\begin{array}{cccccc} \frac{d_{pk}}{l_{ck}} & 0 & 0 & 0 & -\frac{1}{l_{ck}} & 0 \\ 0 & \frac{d_{pk}}{l_{ck}} & 0 & \frac{1}{l_{ck}} & 0 & 0 \\ \multicolumn{6}{c}{\mathbf{0}_{3\times 6}} \\ 0 & 0 & 0 & 0 & 0 & 1 \end{array}\right] \tag{54}$$

$$\mathbf{S}_{bpk} = \left[\begin{array}{cccccc} \frac{d_{bk}}{l_{ck}} & 0 & 0 & 0 & \frac{1}{l_{ck}} & 0 \\ 0 & \frac{d_{bk}}{l_{ck}} & 0 & -\frac{1}{l_{ck}} & 0 & 0 \\ \multicolumn{6}{c}{\mathbf{0}_{4\times 6}} \end{array}\right], \quad \mathbf{S}_{ppk} = \left[\begin{array}{cccccc} \frac{l_{ck}-d_{pk}}{l_{ck}} & 0 & 0 & 0 & \frac{1}{l_{ck}} & 0 \\ 0 & \frac{l_{ck}-d_{pk}}{l_{ck}} & 0 & -\frac{1}{l_{ck}} & 0 & 0 \\ 0 & 0 & 1 & 0 & 0 & 0 \\ \multicolumn{6}{c}{\mathbf{0}_{3\times 6}} \end{array}\right] \tag{55}$$

and $l_{ck} = l_{bk} + q_k$ is a total length of the cylinder k.

4.3. Determination of reaction wrenches

The reaction wrench in Joint k (the revolute joint of Link k) is determined by

$$\mathrm{W}_{\mathrm{r}\,k}^{\,k} = \sum_{j=k}^{n}\mathbf{U}^{k}_{k,m_j}\bar{\mathbf{R}}^{k}_{j}(-\mathrm{W}_{\mathrm{t}\,j}^{\,j}) + \sum_{j=k}^{n}\mathbf{U}^{k}_{k,P_j}\bar{\mathbf{R}}^{k}_{pj}(-\mathrm{W}^{*\,pj}_{\mathrm{t}\,pj}) + \sum_{j=k+1}^{n}\mathbf{U}^{k}_{k,bj}\bar{\mathbf{R}}^{k}_{bj}(-\mathrm{W}^{*\,bj}_{\mathrm{t}\,bj}), \tag{56}$$

where $\mathbf{U}^{a}_{ab}$ are the screw reference transformation matrices as in (19), $\bar{\mathbf{R}}^{a}_{b}$ are the screw coordinate transformation matrices as in (21), where the frame notations are as given in Fig. 4. The wrenches $\mathrm{W}_{\mathrm{t}\,j}^{\,j}$ are given by (49) and (50), while the wrenches $\mathrm{W}^{*\,pj}_{\mathrm{t}\,pj}$, $\mathrm{W}^{*\,bj}_{\mathrm{t}\,bj}$ are given by (53). The point P_j is the piston pj attachment point to Link j, the point bj is the origin of Frame bj.

5. Knuckle boom crane

5.1. Dynamic modelling

Knuckle boom cranes are often installed on offshore vessels and they continuously experience significant dynamic loads. Therefore, the reaction forces should be determined taking into account inertial loads from the dynamic analysis. In this work we assume that a crane is fixed to a stationary base and a payload is omitted, however it is straightforward to extend the presented procedure and include the payload and the base motion [6,30]. Consider a crane system given in Fig. 5. The dynamical system consists of seven rigid bodies: Body 1 is the crane king, Body 2 and Body 3 are the crane booms, Body $b2$ and Body $p2$ are the barrel and the piston of the inner cylinder, Body $b3$ and Body $p3$ are the barrel and the piston of the outer cylinder. Each Body i has a body-fixed Frame i, while the inertial frame is denoted Frame 0. Note that x_i axes for some of the frames are not shown in Fig. 5, they are defined by the right hand rule. The configuration of the crane is defined by three generalized coordinates: q_1 is the rotation angle of the king about z_0 axis, q_2 is the piston extension of the inner cylinder and q_3 is the piston extension of the outer cylinder. Then the configuration space vector $\mathbf{q}$ and the generalized speed vector $\mathbf{u}$ are defined as

$$\mathbf{q} = \begin{bmatrix} q_1 & q_2 & q_3 \end{bmatrix}^{\mathrm{T}}, \quad \mathbf{u} = \begin{bmatrix} u_1 & u_2 & u_3 \end{bmatrix}^{\mathrm{T}}. \tag{57}$$

The rotation matrix from Frame 0 to Frame 1 is $\mathbf{R}^{0}_{1} = \mathbf{R}_z(q_1)$, the rotation matrix from Frame 1 to Frame 2 is $\mathbf{R}^{1}_{2} = \mathbf{R}_x(\alpha_2(q_2))$, the rotation matrix from Frame 2 to Frame 3 is $\mathbf{R}^{2}_{3} = \mathbf{R}_x(\alpha_3(q_3))$, where $\alpha_2(q_2)$ and $\alpha_3(q_3)$ are given by (29). The rotation matrix from Frame 1 to Frame $b2$ is $\mathbf{R}^{1}_{b2} = \mathbf{R}_x(\beta_2(q_2))$, the rotation matrix from Frame 2 to Frame $b3$ is $\mathbf{R}^{2}_{b3} = \mathbf{R}_x(\beta_3(q_3))$, where $\beta_2(q_2)$ and $\beta_3(q_3)$ are given by (30). The rotation matrices from Frame $b2$/$b3$ to Frame $p2$/$p3$ are $\mathbf{R}^{b2}_{p2} = \mathbf{R}^{b3}_{p3} = \mathbf{I}$.

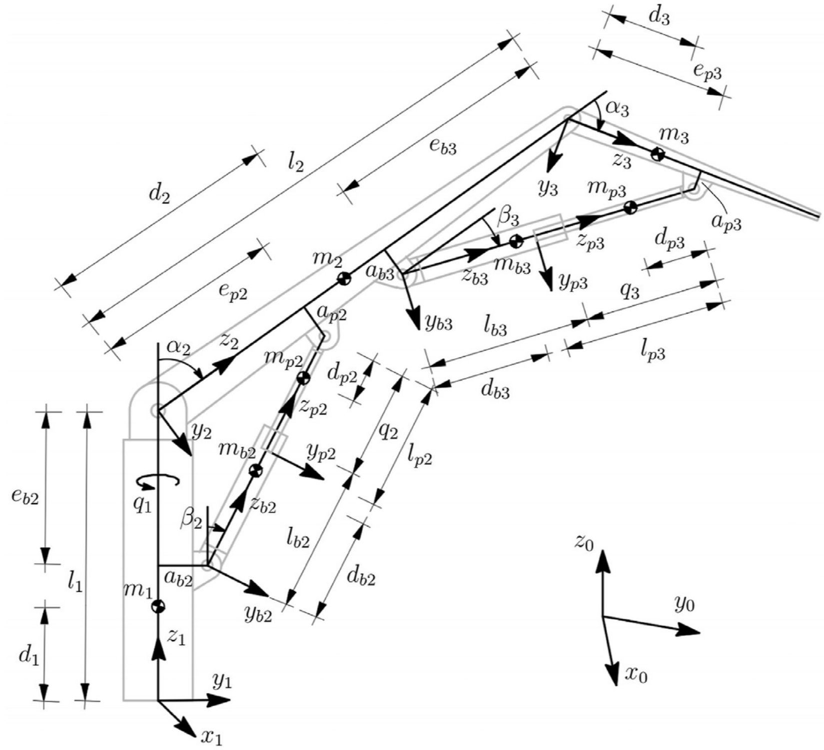

Fig. 5. A knuckle boom crane system without a payload.

The relative twists between the system bodies are defined as

$$\begin{aligned}
\mathrm{t}^1_{01/1} &= \begin{bmatrix} 0 & 0 & u_1 & \mathbf{0}_{1\times3} \end{bmatrix}^{\mathrm{T}}, \quad \mathrm{t}^2_{12/2} = \begin{bmatrix} \dot{\alpha}_2 & 0 & 0 & \mathbf{0}_{1\times3} \end{bmatrix}^{\mathrm{T}}, \quad \mathrm{t}^3_{23/3} = \begin{bmatrix} \dot{\alpha}_3 & 0 & 0 & \mathbf{0}_{1\times3} \end{bmatrix}^{\mathrm{T}}, \\
\mathrm{t}^{b2}_{1,b2/b2} &= \begin{bmatrix} \dot{\beta}_2 & 0 & 0 & \mathbf{0}_{1\times3} \end{bmatrix}^{\mathrm{T}}, \quad \mathrm{t}^{p2}_{b2,p2/p2} = \begin{bmatrix} \mathbf{0}_{1\times3} & 0 & 0 & u_2 \end{bmatrix}^{\mathrm{T}}, \\
\mathrm{t}^{b3}_{2,b3/b3} &= \begin{bmatrix} \dot{\beta}_3 & 0 & 0 & \mathbf{0}_{1\times3} \end{bmatrix}^{\mathrm{T}}, \quad \mathrm{t}^{p3}_{b3,p3/p3} = \begin{bmatrix} \mathbf{0}_{1\times3} & 0 & 0 & u_3 \end{bmatrix}^{\mathrm{T}},
\end{aligned} \tag{58}$$

where $\dot{\alpha}_i$ and $\dot{\beta}_i$ are given by (37) and (40).

The twist t^1_{01/m_1} referenced to the COG of Body 1, relative to the inertial frame and expressed in the coordinates of Frame 1 is

$$\mathrm{t}^1_{01/m_1} = \mathbf{U}^1_{m_1,1}\mathrm{t}^1_{01/1}. \tag{59}$$

The twist t^2_{02/m_2} referenced to the COG of Body 2, relative to the inertial frame and expressed in the coordinates of Frame 2 is

$$\mathrm{t}^2_{01/m_2} = \mathbf{V}^{21}_{m_2,1}\mathrm{t}^1_{01/1}, \quad \mathrm{t}^2_{12/m_2} = \mathbf{U}^2_{m_2,2}\mathrm{t}^2_{12/2}, \quad \mathrm{t}^2_{02/m_2} = \mathrm{t}^2_{01/m_2} + \mathrm{t}^2_{12/m_2}. \tag{60}$$

The twist t^3_{03/m_3} referenced to the COG of Body 3, relative to the inertial frame and expressed in the coordinates of Frame 3 is

$$\begin{aligned}
\mathrm{t}^2_{02/2} &= \mathbf{U}^2_{2,m_2}\mathrm{t}^2_{02/m_2}, \quad \mathrm{t}^3_{02/m_3} = \mathbf{V}^{32}_{m_3,2}\mathrm{t}^2_{02/2}, \\
\mathrm{t}^3_{23/m_3} &= \mathbf{U}^3_{m_3,3}\mathrm{t}^3_{23/3}, \quad \mathrm{t}^3_{03/m_3} = \mathrm{t}^3_{02/m_3} + \mathrm{t}^3_{23/m_3}.
\end{aligned} \tag{61}$$

The twist $\mathrm{t}^{b2}_{0,b2/m_{b2}}$ referenced to the COG of Body $b2$, relative to the inertial frame and expressed in the coordinates of Frame $b2$ is

$$\mathrm{t}^{b2}_{01/m_{b2}} = \mathbf{V}^{b2,1}_{m_{b2},1}\mathrm{t}^1_{01/1}, \quad \mathrm{t}^{b2}_{1,b2/m_{b2}} = \mathbf{U}^{b2}_{m_{b2},b2}\mathrm{t}^{b2}_{1,b2/b2}, \quad \mathrm{t}^{b2}_{0,b2/m_{b2}} = \mathrm{t}^{b2}_{01/m_{b2}} + \mathrm{t}^{b2}_{1,b2/m_{b2}}. \tag{62}$$

The twist $\mathrm{t}^{p2}_{0,p2/m_{p2}}$ referenced to the COG of Body $p2$, relative to the inertial frame and expressed in the coordinates of Frame $p2$ is

$$\begin{aligned}&\mathrm{t}^{b2}_{0,b2/b2} = \mathbf{U}^{b2}_{b2,m_{b2}}\mathrm{t}^{b2}_{0,b2/m_{b2}}, \quad \mathrm{t}^{p2}_{0,b2/m_{p2}} = \mathbf{V}^{p2,b2}_{m_{p2},b2}\mathrm{t}^{b2}_{0,b2/b2},\\ &\mathrm{t}^{p2}_{b2,p2/m_{p2}} = \mathbf{U}^{p2}_{m_{p2},p2}\mathrm{t}^{p2}_{b2,p2/p2}, \quad \mathrm{t}^{p2}_{0,p2/m_{p2}} = \mathrm{t}^{p2}_{0,b2/m_{p2}} + \mathrm{t}^{p2}_{b2,p2/m_{p2}}.\end{aligned} \tag{63}$$

The twist $\mathrm{t}^{b3}_{0,b3/m_{b3}}$ referenced to the COG of Body $b3$, relative to the inertial frame and expressed in the coordinates of Frame $b3$ is

$$\mathrm{t}^{b3}_{02/m_{b3}} = \mathbf{V}^{b3,2}_{m_{b3},2}\mathrm{t}^{2}_{02/2}, \quad \mathrm{t}^{b3}_{2,b3/m_{b3}} = \mathbf{U}^{b3}_{m_{b3},b3}\mathrm{t}^{b3}_{2,b3/b3}, \quad \mathrm{t}^{b3}_{0,b3/m_{b3}} = \mathrm{t}^{b3}_{02/m_{b3}} + \mathrm{t}^{b3}_{2,b3/m_{b3}}. \tag{64}$$

The twist $\mathrm{t}^{p3}_{0,p3/m_{p3}}$ referenced to the COG of Body $p3$, relative to the inertial frame and expressed in the coordinates of Frame $p3$ is

$$\begin{aligned}&\mathrm{t}^{b3}_{0,b3/b3} = \mathbf{U}^{b3}_{b3,m_{b3}}\mathrm{t}^{b3}_{0,b3/m_{b3}}, \quad \mathrm{t}^{p3}_{0,b3/m_{p3}} = \mathbf{V}^{p3,b3}_{m_{p3},b3}\mathrm{t}^{b3}_{0,b3/b3},\\ &\mathrm{t}^{p3}_{b3,p3/m_{p3}} = \mathbf{U}^{p3}_{m_{p3},p3}\mathrm{t}^{p3}_{b3,p3/p3}, \quad \mathrm{t}^{p3}_{0,p3/m_{p3}} = \mathrm{t}^{p3}_{0,b3/m_{p3}} + \mathrm{t}^{p3}_{b3,p3/m_{p3}}.\end{aligned} \tag{65}$$

The projection matrices $\mathbf{P}_k$ for the links, $\mathbf{P}_{bk}$ for the cylinder barrels and $\mathbf{P}_{pk}$ for the cylinder pistons can now be calculated by (28).

The inertia tensors are assumed to be

$$\begin{aligned}\mathbf{M}^1_{m_1} &= \mathrm{diag}(m_1 l_1^2/12,\ m_1 l_1^2/12,\ 0.1 m_1 l_1^2/12),\\ \mathbf{M}^k_{m_k} &= \mathrm{diag}(m_k l_k^2/12,\ m_k l_k^2/12,\ 0) \quad \text{for } k = 2, 3,\\ \mathbf{M}^{bk}_{m_{bk}} &= \mathrm{diag}(m_{bk} l_{bk}^2/12,\ m_{bk} l_{bk}^2/12,\ 0) \quad \text{for } k = 2, 3,\\ \mathbf{M}^{pk}_{m_{pk}} &= \mathrm{diag}(m_{pk} l_{pk}^2/12,\ m_{pk} l_{pk}^2/12,\ 0) \quad \text{for } k = 2, 3.\end{aligned} \tag{66}$$

where, except for Link 1, all bodies in the system are assumed to be slender beams. The matrices $\mathbf{D}_k$, $\mathbf{D}_{bk}$, $\mathbf{D}_{pk}$, $\mathbf{W}_k$, $\mathbf{W}_{bk}$ and $\mathbf{W}_{pk}$ are calculated by (45), provided that $\boldsymbol{\omega}^k_{0k}$, $\boldsymbol{\omega}^{bk}_{0,bk}$ and $\boldsymbol{\omega}^{pk}_{0,pk}$ are the first three rows of the twists t^k_{0k/m_k}, $\mathrm{t}^{bk}_{0,bk/m_{bk}}$ and $\mathrm{t}^{pk}_{0,pk/m_{pk}}$ respectively.

The wrenches of external forces applied at the COG of each body are

$$\mathrm{W_e}^1_1 = \begin{bmatrix} \mathbf{R}^1_0\begin{bmatrix}0\\0\\-m_1 g\end{bmatrix}\\ 0\\ 0\\ T_1\end{bmatrix}, \quad \mathrm{W_e}^k_k = \begin{bmatrix} \mathbf{R}^k_0\begin{bmatrix}0\\0\\-m_k g\end{bmatrix}\\ 0\\ 0\\ 0\end{bmatrix} \tag{67}$$

and

$$\mathrm{W_e}^{bk}_{bk} = \begin{bmatrix} \mathbf{R}^{bk}_0\begin{bmatrix}0\\0\\-m_{bk} g\end{bmatrix} + \begin{bmatrix}0\\0\\-F_k\end{bmatrix}\\ \mathbf{0}_{3\times1}\end{bmatrix}, \quad \mathrm{W_e}^{pk}_{pk} = \begin{bmatrix} \mathbf{R}^{pk}_0\begin{bmatrix}0\\0\\-m_{pk} g\end{bmatrix} + \begin{bmatrix}0\\0\\F_k\end{bmatrix}\\ \mathbf{0}_{3\times1}\end{bmatrix}, \tag{68}$$

where $k = 2, 3$, $\mathbf{R}^i_0 = (\mathbf{R}^0_i)^{\mathrm{T}}$, T_1 is the actuation torque of the crane king, F_k is the piston pk actuation force and g is the acceleration of gravity. After the vector of generalized external forces $\boldsymbol{\tau}$ is calculated by (46), the equation of motion (43) for the crane can be finally formulated.

5.2. Reaction forces

The reaction forces in Joint 1 (the revolute joint of Link 1) are determined by (56)

$$\begin{aligned}\mathrm{W_r}^1_1 =& \mathbf{U}^1_{1,m_1}(-\mathrm{W_t}^1_1) + \mathbf{U}^1_{1,m_2}\bar{\mathbf{R}}^1_2(-\mathrm{W_t}^2_2) + \mathbf{U}^1_{1,m_3}\bar{\mathbf{R}}^1_3(-\mathrm{W_t}^3_3)\\ &+ \mathbf{U}^1_{1,P_2}\bar{\mathbf{R}}^1_{p2}(-\mathrm{W}^{*\,p2}_{\mathrm{t}\,p2}) + \mathbf{U}^1_{1,P_3}\bar{\mathbf{R}}^1_{p3}(-\mathrm{W}^{*\,p3}_{\mathrm{t}\,p3})\\ &+ \mathbf{U}^1_{1,b2}\bar{\mathbf{R}}^1_{b2}(-\mathrm{W}^{*\,b2}_{\mathrm{t}\,b2}) + \mathbf{U}^1_{1,b3}\bar{\mathbf{R}}^1_{b3}(-\mathrm{W}^{*\,b3}_{\mathrm{t}\,b3}),\end{aligned} \tag{69}$$

Table 1
System parameters.

Length	l_1	l_2	l_3	l_{b2}	l_{p2}	l_{b3}	l_{p3}	
Value, m	6.0	7.5	5.0	2.3	2.0	2.3	2.0	
COG distance	d_1	d_2	d_3	d_{b2}	d_{p2}	d_{b3}	d_{p3}	
Value, m	3.0	3.7	2.5	1.2	1.2	1.2	1.2	
Offset	e_{b2}	e_{p2}	e_{b3}	e_{p3}	a_{b2}	a_{p2}	a_{b3}	a_{p3}
Value, m	2.5	2.5	2.5	2.0	1.0	0.5	0.4	0.4

where the wrenches $\mathrm{W_t}{}_i^i$, $\mathrm{W}^{*}{}_{t\,pi}^{pi}$ and $\mathrm{W}^{*}{}_{t\,bi}^{bi}$ are given by (49), (50) and (53). The position vectors for the screw reference transformation matrices are defined as follows

$$\begin{aligned}
\mathbf{U}_{1,m_1}^1 :&\quad \mathbf{p}_{1,m_1}^1 = \begin{bmatrix}0 & 0 & d_1\end{bmatrix}^\mathrm{T},\\
\mathbf{U}_{1,m_2}^1 :&\quad \mathbf{p}_{1,m_2}^1 = \begin{bmatrix}0 & 0 & l_1\end{bmatrix}^\mathrm{T} + \mathbf{R}_2^1\begin{bmatrix}0 & 0 & d_2\end{bmatrix}^\mathrm{T},\\
\mathbf{U}_{1,m_3}^1 :&\quad \mathbf{p}_{1,m_3}^1 = \begin{bmatrix}0 & 0 & l_1\end{bmatrix}^\mathrm{T} + \mathbf{R}_2^1\begin{bmatrix}0 & 0 & l_2\end{bmatrix}^\mathrm{T} + \mathbf{R}_3^1\begin{bmatrix}0 & 0 & d_3\end{bmatrix}^\mathrm{T},\\
\mathbf{U}_{1,P_2}^1 :&\quad \mathbf{p}_{1,P_2}^1 = \begin{bmatrix}0 & 0 & l_1\end{bmatrix}^\mathrm{T} + \mathbf{R}_2^1\begin{bmatrix}0 & a_{p2} & e_{p2}\end{bmatrix}^\mathrm{T},\\
\mathbf{U}_{1,P_3}^1 :&\quad \mathbf{p}_{1,P_3}^1 = \begin{bmatrix}0 & 0 & l_1\end{bmatrix}^\mathrm{T} + \mathbf{R}_2^1\begin{bmatrix}0 & 0 & l_2\end{bmatrix}^\mathrm{T} + \mathbf{R}_3^1\begin{bmatrix}0 & a_{p3} & e_{p3}\end{bmatrix}^\mathrm{T},\\
\mathbf{U}_{1,b2}^1 :&\quad \mathbf{p}_{1,b2}^1 = \begin{bmatrix}0 & a_{b2} & l_1 - e_{b2}\end{bmatrix}^\mathrm{T},\\
\mathbf{U}_{1,b3}^1 :&\quad \mathbf{p}_{1,b3}^1 = \begin{bmatrix}0 & 0 & l_1\end{bmatrix}^\mathrm{T} + \mathbf{R}_2^1\begin{bmatrix}0 & a_{b3} & l_2 - e_{b3}\end{bmatrix}^\mathrm{T}.
\end{aligned} \tag{70}$$

The reaction forces in Joint 2 (the revolute joint of Link 2) are determined by (56)

$$\begin{aligned}
\mathrm{W_r}{}_2^2 =& \mathbf{U}_{2,m_2}^2(-\mathrm{W_t}{}_2^2) + \mathbf{U}_{2,m_3}^2\bar{\mathbf{R}}_3^2(-\mathrm{W_t}{}_3^3)\\
&+ \mathbf{U}_{2,P_2}^2\bar{\mathbf{R}}_{p2}^2(-\mathrm{W}^{*}{}_{t\,p2}^{p2}) + \mathbf{U}_{2,P_3}^2\bar{\mathbf{R}}_{p3}^2(-\mathrm{W}^{*}{}_{t\,p3}^{p3})\\
&+ \mathbf{U}_{2,b3}^2\bar{\mathbf{R}}_{b3}^2(-\mathrm{W}^{*}{}_{t\,b3}^{b3}),
\end{aligned} \tag{71}$$

where the wrenches $\mathrm{W_t}{}_i^i$, $\mathrm{W}^{*}{}_{t\,pi}^{pi}$ and $\mathrm{W}^{*}{}_{t\,bi}^{bi}$ are given by (49), (50) and (53). The position vectors for the screw reference transformation matrices are defined as follows

$$\begin{aligned}
\mathbf{U}_{2,m_2}^2 :&\quad \mathbf{p}_{2,m_2}^2 = \begin{bmatrix}0 & 0 & d_2\end{bmatrix}^\mathrm{T},\\
\mathbf{U}_{2,m_3}^2 :&\quad \mathbf{p}_{2,m_3}^2 = \begin{bmatrix}0 & 0 & l_2\end{bmatrix}^\mathrm{T} + \mathbf{R}_3^2\begin{bmatrix}0 & 0 & d_3\end{bmatrix}^\mathrm{T},\\
\mathbf{U}_{2,P_2}^2 :&\quad \mathbf{p}_{2,P_2}^2 = \begin{bmatrix}0 & a_{p2} & e_{p2}\end{bmatrix}^\mathrm{T},\\
\mathbf{U}_{2,P_3}^2 :&\quad \mathbf{p}_{2,P_3}^2 = \begin{bmatrix}0 & 0 & l_2\end{bmatrix}^\mathrm{T} + \mathbf{R}_3^2\begin{bmatrix}0 & a_{p3} & e_{p3}\end{bmatrix}^\mathrm{T},\\
\mathbf{U}_{2,b3}^2 :&\quad \mathbf{p}_{2,b3}^2 = \begin{bmatrix}0 & a_{b3} & l_2 - e_{b3}\end{bmatrix}^\mathrm{T}.
\end{aligned} \tag{72}$$

The reaction forces in Joint 3 (the revolute joint of Link 3) can now similarly be determined by (56)

$$\mathrm{W_r}{}_3^3 = \mathbf{U}_{3,m_3}^3(-\mathrm{W_t}{}_3^3) + \mathbf{U}_{3,P_3}^3\bar{\mathbf{R}}_{p3}^3(-\mathrm{W}^{*}{}_{t\,p3}^{p3}), \tag{73}$$

where the wrenches $\mathrm{W_t}{}_3^3$ and $\mathrm{W}^{*}{}_{t\,p3}^{p3}$ are given by (49), (50) and (53), and the position vectors for the screw reference transformation matrices are defined as follows

$$\begin{aligned}
\mathbf{U}_{3,m_3}^3 :&\quad \mathbf{p}_{3,m_3}^3 = \begin{bmatrix}0 & 0 & d_3\end{bmatrix}^\mathrm{T},\\
\mathbf{U}_{3,P_3}^3 :&\quad \mathbf{p}_{3,P_3}^3 = \begin{bmatrix}0 & a_{p3} & e_{p3}\end{bmatrix}^\mathrm{T}.
\end{aligned} \tag{74}$$

6. Simulation results

The knuckle boom crane model from the previous section is computationally implemented and the results of the numerical simulation are presented in this section. The crane parameters and masses used in the simulation are given in Tables 1 and 2.

The crane is controlled by the PD controller with gravity compensation. As the control scheme is not the goal of this work, we will not go into the details of the control scheme. The defined motion path represents a typical sequence of crane configurations during a hoisting operation.

Table 2
System masses.

Mass	m_1	m_2	m_3	m_{b2}	m_{p2}	m_{b3}	m_{p3}
Value, t	10.0	10.0	10.0	2.0	1.0	2.0	1.0

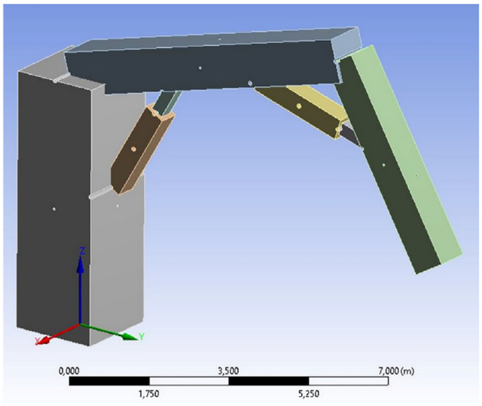

Fig. 6. ANSYS model of the knuckle boom crane.

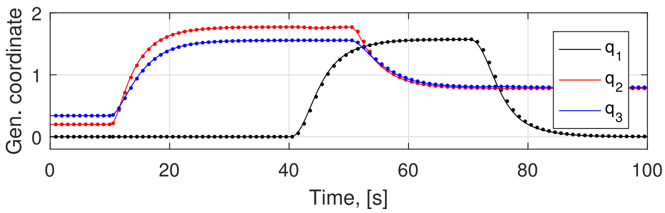

Fig. 7. Generalized coordinates, given in [m] or [rad].

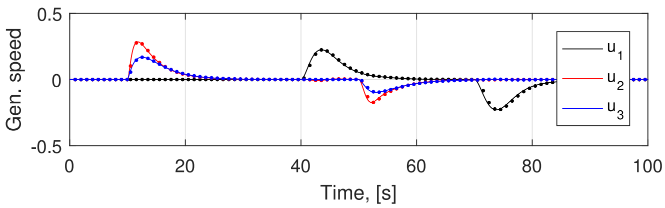

Fig. 8. Generalized speeds, given in [m/s] or [rad/s].

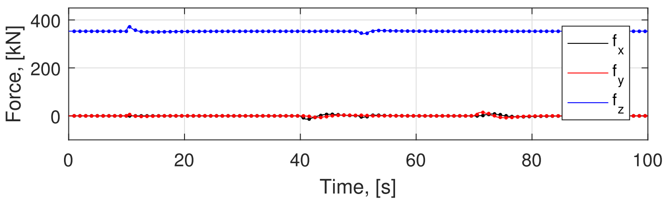

Fig. 9. Reaction forces in Joint 1, given in the coordinates of Frame 0.

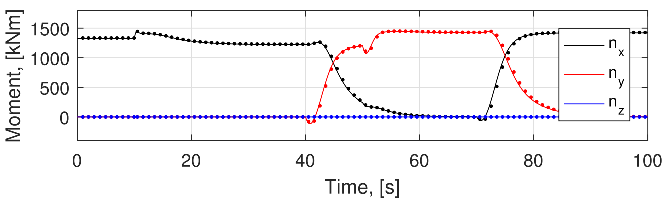

Fig. 10. Reaction moments in Joint 1, given in the coordinates of Frame 0.

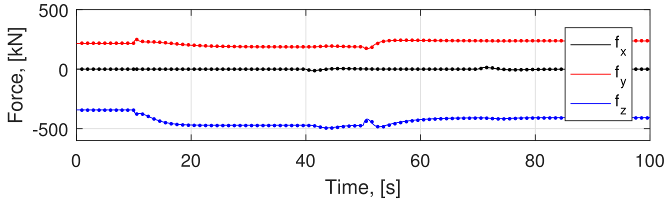

Fig. 11. Reaction forces in Joint 2, given in the coordinates of Frame 2.

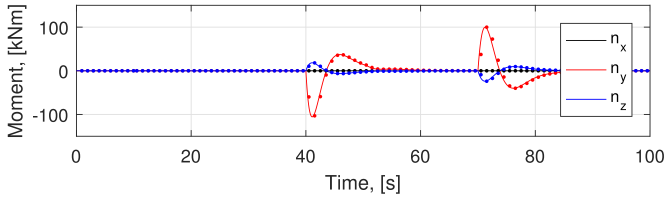

Fig. 12. Reaction moments in Joint 2, given in the coordinates of Frame 2.

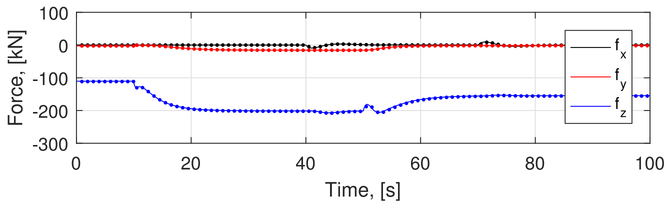

Fig. 13. Reaction forces in Joint 3, given in the coordinates of Frame 3.

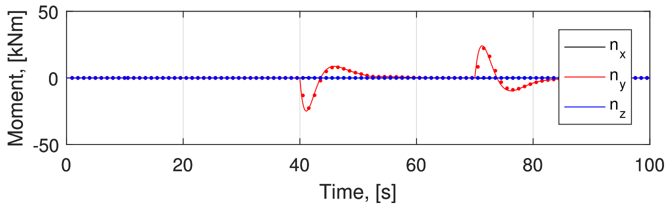

Fig. 14. Reaction moments in Joint 3, given in the coordinates of Frame 3.

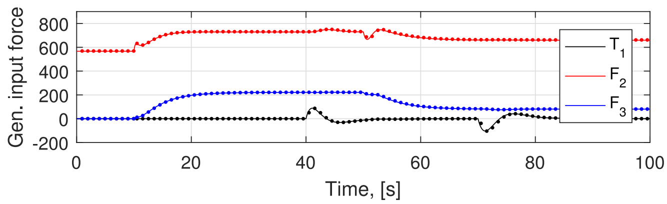

Fig. 15. Generalized input forces, given in [kN] or [kNm].

The values of the generalized coordinates and the generalized speeds during the simulation are given in Figs. 7 and 8. The reaction forces and moments in Joint 1, given in the coordinates of Frame 0 are shown in Figs. 9 and 10. The reaction forces and moments in Joint 2, given in the coordinates of Frame 2 are shown in Fig. 11 and 12. The reaction forces and moments in Joint 3, given in the coordinates of Frame 3 are shown in Fig. 13 and 14. The actuator input forces and torques are given in Fig. 15.

The reaction forces in the joints are validated by the results obtained using Rigid Dynamics module in ANSYS, see Fig. 6. The time histories of the generalized speeds (see Fig. 8) were used as input velocities for the ANSYS model. Mechanical and inertial properties of the bodies in the model are according to Tables 1 and 2. The results from ANSYS are shown with a "•" symbol in the graphs, while the results obtained by (69), (71) and (73) are shown with solid lines. The time histories given in Figs. 9–14 show good agreement with the results obtained from the ANSYS analysis. The moment n_x in the passive joints (Joints 2 and 3) is equal to zero throughout the simulations, which agrees with the mechanical arrangement of the crane.

7. Conclusions

We have presented the method for dynamic force analysis of a knuckle boom crane. The method was presented in a general manner and can be applied for crane-like manipulators with an arbitrary number of links. Both dynamic modelling and force analysis procedures were derived using screws and screw transformations, which led to the efficient and geometrically meaningful formulation. The detailed implementation of the method was demonstrated for a specific case of a knuckle boom crane, where the reaction forces for three joints of the crane were determined. The numerical simulation was carried out and the results were provided. The magnitudes of the reaction forces showed good agreement with the values obtained by the independent dynamic analysis in ANSYS.

It is proposed that further development of this work could be the implementation of the force analysis method for a coupled crane and marine vessel model. Such model could provide an important contribution to solving dry friction compensation and mechanical design problems for offshore cranes in practice.

Acknowledgment

The research presented in this paper has received funding from the Norwegian Research Council, SFI Offshore Mechatronics, project number 237896.

References

[1] L. Ramli, Z. Mohamed, A.M. Abdullahi, H. Jaafar, I.M. Lazim, Control strategies for crane systems: a comprehensive review, Mech. Syst. Signal Process. 95 (2017) 1–23.
[2] E.M. Abdel-Rahman, A.H. Nayfeh, Z.N. Masoud, Dynamics and control of cranes: a review, Modal Anal. 9 (7) (2003) 863–908.
[3] M. Linjama, T. Virvalo, Low-order dynamic model for flexible hydraulic cranes, Proc. Inst. Mech. Eng. Part I J. Syst. Control Eng. 213 (1) (1999) 11–22.
[4] R. Bianchi, G.F. Ritelli, A. Vacca, Payload oscillation reduction in load-handling machines: a frequency-based approach, Proc. Inst. Mech. Eng. Part I J. Syst. Control Eng. 231 (3) (2017) 199–212.
[5] M.K. Bak, M.R. Hansen, Analysis of offshore knuckle boom crane-part one: modeling and parameter identification, Model. Identif. Control 34 (4) (2013) 157.
[6] G.O. Tysse, O. Egeland, Dynamic interaction of a heavy crane and a ship in wave motion, J. Model. Identif. Control 39 (2) (2018) 45–60.
[7] M. Agostini, G.G. Parker, K. Groom, H. Schaub, R.D. Robinett, Command shaping and closed-loop control interactions for a ship crane, in: Proceedings of the American Control Conference, 2002, Vol. 3, IEEE, 2002, pp. 2298–2304.
[8] E.D. Stoenescu, D.B. Marghitu, Effect of prismatic joint inertia on dynamics of kinematic chains, Mech. Mach. Theory 39 (4) (2004) 431–443.
[9] G. Song, L. Cai, Y. Wang, Robust friction compensation for precise and smooth position regulation, Proc. Inst. Mech. Eng. Part I J. Syst. Control Eng. 213 (2) (1999) 157–161.
[10] K. Papakostas, S. Mouroutsos, B. Porter, Genetic design of dynamically optimal robotic manipulators, Proc. Inst. Mech. Eng. Part I J. Syst. Control Eng. 212 (6) (1998) 423–436.
[11] B. Siciliano, L. Sciavicco, L. Villani, G. Oriolo, Robotics: Modelling, Planning and Control, 1st, Springer Publishing Company, Incorporated, 2008.
[12] J. Luh, W. MW, P. RC, On-line computational scheme for mechanical manipulators, ASME. J. Dyn. Sys. Meas. Control. 102 (2) (1980) 69–76.
[13] T.R. Kane, D.A. Levinson, Dynamics, Theory and Applications, McGraw Hill, 1985.
[14] S. Šalinić, G. Bošković, M. Nikolić, Dynamic modelling of hydraulic excavator motion using Kane's equations, Autom. Constr. 44 (2014) 56–62.
[15] S. Agrawal, Multibody dynamics: a formulation using Kanes method and dual vectors, J. Mech. Des. 115 (4) (1993) 833–838.
[16] J. Angeles, S.K. Lee, The formulation of dynamical equations of holonomic mechanical systems using a natural orthogonal complement, J. Appl. Mech. 55 (1988) 243.
[17] J. Angeles, O. Ma, Dynamic simulation of n-axis serial robotic manipulators using a natural orthogonal complement, Int. J. Rob. Res. 7 (5) (1988) 32–47.
[18] S.K. Saha, A decomposition of the manipulator inertia matrix, IEEE Trans. Robot. Autom. 13 (2) (1997) 301–304.
[19] S.K. Saha, Dynamics of serial multibody systems using the decoupled natural orthogonal complement matrices, J. Appl. Mech. 66 (4) (1999) 986–996.
[20] S. Šalinić, Determination of joint reaction forces in a symbolic form in rigid multibody systems, Mech. Mach. Theory 46 (11) (2011) 1796–1810.
[21] C. Dhanaraj, A.M. Sharan, Efficient modeling of rigid link robot dynamic problems with friction, Mech. Mach. Theory 30 (5) (1995) 749–764.
[22] R. Huston, Constraint forces and undetermined multipliers in constrained multibody systems, Multibody Syst. Dyn. 3 (4) (1999) 381–389.
[23] G. Pennock, A. Yang, Dynamic analysis of a multi-rigid-body open-chain system, J. Mech. Trans. Autom. Des. 105 (1) (1983) 28–34.
[24] F. Marques, A.P. Souto, P. Flores, On the constraints violation in forward dynamics of multibody systems, Multibody Syst. Dyn. 39 (4) (2017) 385–419.
[25] M. Wojtyra, Joint reactions in rigid body mechanisms with dependent constraints, Mech. Mach. Theory 44 (12) (2009) 2265–2278.
[26] C.M. Pappalardo, D. Guida, On the lagrange multipliers of the intrinsic constraint equations of rigid multibody mechanical systems, Arch. Appl. Mech. 88 (3) (2018) 419–451.
[27] A. Callejo, F. Gholami, A. Enzenhöfer, J. Kövecses, Unique minimum norm solution to redundant reaction forces in multibody systems, Mech. Mach. Theory 116 (2017) 310–325.
[28] P.K. Eskandary, J. Angeles, The dynamics of a parallel schönflies-motion generator, Mech. Mach. Theory 119 (2018) 119–129.
[29] P.K. Eskandary, J. Angeles, The translating π-joint: design and applications, Mech. Mach. Theory 122 (2018) 361–370.
[30] A. Cibicik, O. Egeland, Determination of constraint forces for an offshore crane on a moving base, in: Proceedings of the 5th International Conference on Control, Decision and Information Technologies (CoDIT), IEEE, 2018, pp. 233–240.
[31] M. Wojtyra, Modeling of static friction in closed-loop kinematic chains uniqueness and parametric sensitivity problems, Multibody Syst. Dyn. 39 (4) (2017) 337–361.
[32] J. Fraczek, M. Wojtyra, On the unique solvability of a direct dynamics problem for mechanisms with redundant constraints and coulomb friction in joints, Mech. Mach. Theory 46 (3) (2011) 312–334.
[33] J.M. McCarthy, G.S. Soh, Geometric design of linkages, Vol. 11, Springer Science & Business Media, 2010.
[34] L. Yanzhu, Screw-matrix method in dynamics of multibody systems, Acta Mech. Sin. 4 (2) (1988) 165–174.
[35] R.M. Murray, S.S. Sastry, L. Zexiang, A mathematical introduction to robotic manipulation, 1st, CRC Press, Inc., Boca Raton, FL, USA, 1994.
[36] H. Liu, T. Huang, A. Kecskeméthy, D.G. Chetwynd, Q. Li, Force/motion transmissibility analyses of redundantly actuated and overconstrained parallel manipulators, Mech. Mach. Theory 109 (2017) 126–138.
[37] O. Egeland, J.R. Sagli, Coordination of motion in a spacecraft/manipulator system, Int. J. Rob. Res. 12 (4) (1993) 366–379.